9th South African Conference on Computational and Applied Mechanics
Somerset West
14 – 16 January 2014

Feasibility of Detecting Cracks in Rail Track at Long Range using Guided Wave Ultrasound

Philip W. Loveday*, Craig S. Long

CSIR Material Science and Manufacturing, South Africa

*PLoveday@csir.co.za

Abstract: A transducer array comprising four transducers was developed and used to perform pulse – echo measurements on a heavy duty welded rail track. A signal processing algorithm, which uses properties of the propagating modes computed using semi-analytical finite element modelling, was developed. The algorithm was used to process the measurement results and a particular mode of propagation proved to be effective. Defects could be detected at long range in relatively new rail while detecting defects in old rail with frequent welded repairs is very difficult. It is expected that transverse cracks in the rail head will be detectable at a range of 500m prior to complete breakage in relatively good condition rail.

Keywords: Guided waves, defect detection, rail track

INTRODUCTION

Guided wave ultrasound has the potential to inspect large portions of a structure from a single transducer location. Pipeline inspection is an example of a successful application of this technology to a one-dimensional waveguide. Welded rail track is a second example of an effectively one-dimensional elastic waveguide that could exploit the long range ability of guided waves.

Inspection of rail track was performed in the UK by Wilcox et al. [1] using an array of transducers wrapped around the track. The system used numerous transducers and could selectively transmit and receive a number of different modes of propagation. Their intention was to inspect rail track under level crossings and a range of only 50m was required. Relatively small defects could be detected and a method of classifying the type of defect was investigated. A completely different approach was followed to develop a guided wave ultrasound based monitoring system in South Africa [2]. This monitoring system was designed to be permanently installed to allow inspection of the entire line every few minutes. This system uses permanently installed piezoelectric ultrasonic transducers spaced approximately 1 km apart in pitch – catch mode. The primary aim was to detect complete breaks in the welded rail track without producing false alarms. The system does sometimes detect a crack prior to complete breakage but in its current form increasing the sensitivity to cracks also increases the likelihood of false alarms. The possibility of combining the two approaches was considered in [3] and a number of questions were raised. Of primary importance was whether cracks could be detected and located at distances compatible with the monitoring system with only an acceptable increase in system complexity and cost per kilometre.

Detecting, locating and possibly monitoring the growth of cracks requires a pulse – echo mode of operation to be added to the system, which in turn requires that a transducer array be used rather than a single transducer at each station. The pitch – catch mode of operation would be retained as it provides the best way to avoid false alarms. The possibility of detecting cracks at a distance of 500 m from a transducer array

comprising only a small number of transducers is investigated experimentally. In this paper the design of a phased array to control the mode and direction of transmission and reception is described followed by experimental field measurements. The signal processing performed on these measurements is discussed before results are presented.

PHASED ARRAY DESIGN

The purpose of using a phased array of transducers, instead of a single transducer, is to allow some control over which modes are excited and sensed and also to transmit or receive preferentially in one direction along the rail. The design of the array requires knowledge of the modes that are to be used in the application. This knowledge is obtained through a combination of numerical modelling and measurement. Analytical models are available for simple waveguides but for the rail we apply the semi-analytical finite element (SAFE) method [4]. The data obtained from this numerical model forms an important input to designing our experimental setup and processing the measured signals.

Previous field measurements were performed using an ultrasonic transducer to excite the rail and a laser vibrometer to measure the response [5][6]. The vertical displacement responses at hundreds of points on the rail were measured and the amplitudes of the propagating modes (calculated by SAFE analysis) were estimated. Measurements were performed at different distances up to 400m from the transducer. These measurements indicated that there are two modes of propagation that travel with relatively low attenuation. These modes are therefore candidates for long range inspection. Figure 1 shows the mode shapes of these two modes computed using SAFE modelling.

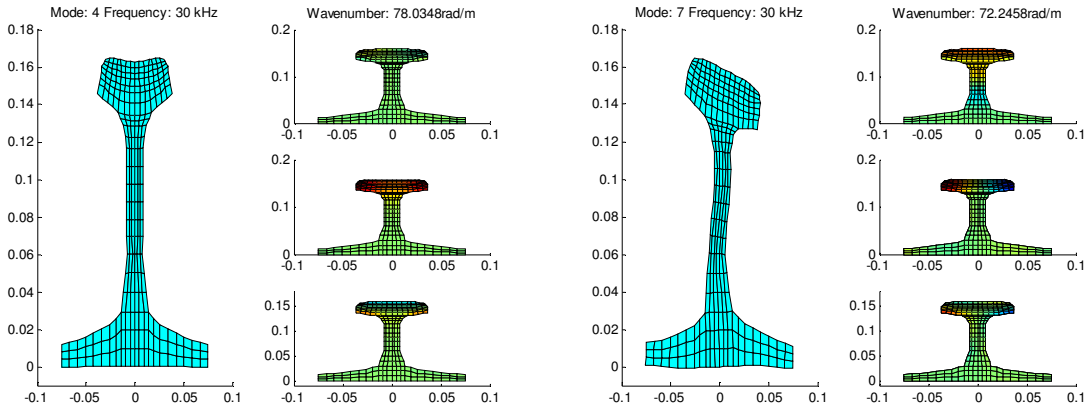

Figure 1 Mode shapes of modes that propagate with relatively low attenuation.

The modes to be used have the feature that the one is symmetric while the other is anti-symmetric with respect to the vertical plane along the rail axis. This means that by positioning two transducers, one on either side of the rail, it will be possible to excite the symmetric mode by driving the two transducers in phase or to excite the anti-symmetric mode by driving them with opposite phase. The same applies for received signals to distinguish between these two modes.

It is possible to excite a mode of propagation in only one direction along the rail. If two transducers are placed at the same position around the circumference but at one quarter wavelength spacing along the rail and the transducers are driven with a 90° phase shift the two excitations cancel in one direction but are added in the other. As the two modes of interest have similar wavenumber (and therefore similar wavelength) we can use two transducers along the rail to control the direction of propagation along the rail. It therefore should be possible to control these two modes and the direction with an array of only four transducers.

If only four transducers are used it is expected that it will not be possible to prevent the excitation and sensing of other propagating modes. If we consider the situation at 30 kHz we have 19 propagating modes

in each direction (forward and backward propagating modes). We can compute what would be sensed by the four transducer array for each of these modes. The signals received by the four element array would be processed into four channels. These sensed modes 1 – 4 correspond to mode 4 forward, mode 7 forward, mode 4 backward and mode 7 backward. The relationship between the four sensed modes and the modes propagating in the rail is illustrated in figure 2. It is seen that the array senses mode 4 forward when this mode is propagating as required. It also senses some of the higher number forward propagating modes (mode 12 and higher), which are also symmetric modes. The second sensing channel, which should sense mode 7 forward does so but also senses other anti-symmetric modes such as modes 6, 8 and 9, which will have similar wavenumbers. It is thought that the rail will filter out the other propagating modes with distance so this should not be a serious problem. An array with a greater number of transducers would be more selective but as we plan to permanently install these arrays we want to keep the number of transducers and therefore cost of the array as low as possible.

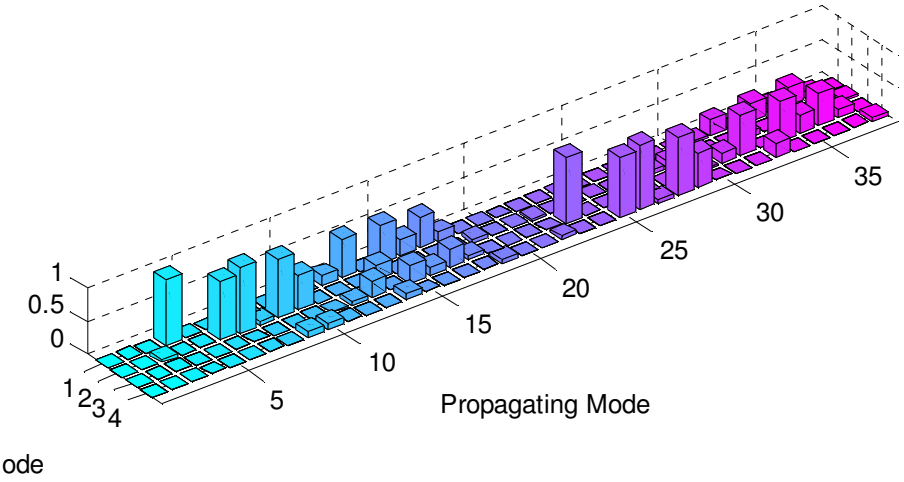

Figure 2 Modes sensed by four element array.

FIELD MEASUREMENTS

Field measurements were performed on an operational heavy duty coal line. Four ultrasonic transducers developed at the CSIR were glued to the UIC60 profile rail as shown in figure 3.

Figure 3 Four transducer array (two transducers hidden on opposite side of rail head)

Diode circuits were used to allow pulse-echo operation. A data acquisition card in a PC was used to generate the excitation signals and to capture the responses. The received signals were sampled at 250 kHz and 2^{17} samples were captured. The average of 20 captured signals was recorded. The transducers were excited with a 17.5 cycle tone burst with 35 kHz centre frequency. Full matrix capture was used as this

requires only one amplifier. The excitation was applied to one transducer at a time while the response of all four transducers was recorded. This resulted in sixteen captured time signals. Typical time signals are shown in figure 4.

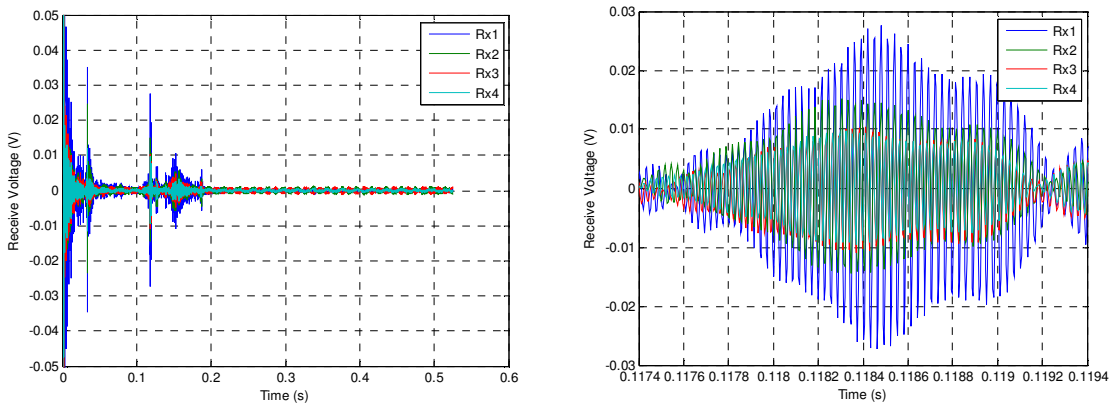

Figure 4 Typical measured signals.

SIGNAL PROCESSING

The captured signals were processed using an algorithm illustrated in figure 5. The algorithm includes functions of removing frequency content (and therefore noise) outside the frequency range of the excitation signal, transducer calibration to take into account the different effectiveness of each transducer, phased array post-processing to combine the signals to effectively excite and sense the targeted modes of propagation. This is performed using knowledge of the modes obtained from the SAFE model. Dispersion compensation is performed using the algorithm introduced by Wilcox [7]. Again, knowledge of the dispersion of the mode computed by the SAFE method is required in this algorithm. Finally deconvolution with the excitation signal is performed, a Hilbert transform is used to obtain the wave packet envelope and the distance traces are scaled to account for attenuation with distance. Particular aspects of the algorithm are described in more detail below.

Phased Array Processing

We assume that the system is linear and we can superimpose signals. Therefore, although the signals were captured by exciting one transducer at a time we can compute the response that would be received (at each transducer) if the transducers had been excited simultaneously with phase differences to excite the two modes of interest in either direction. In addition, we can combine the received signals with phase differences to extract the two modes and directions. This operation is performed in the frequency domain and is represented by equation 1.

$$\alpha(\omega) = R(\omega)^{-1} \cdot S_R(\omega)^{-1} \cdot VR(\omega) \cdot S_T(\omega)^{-1} \cdot R(\omega) \tag{1}$$

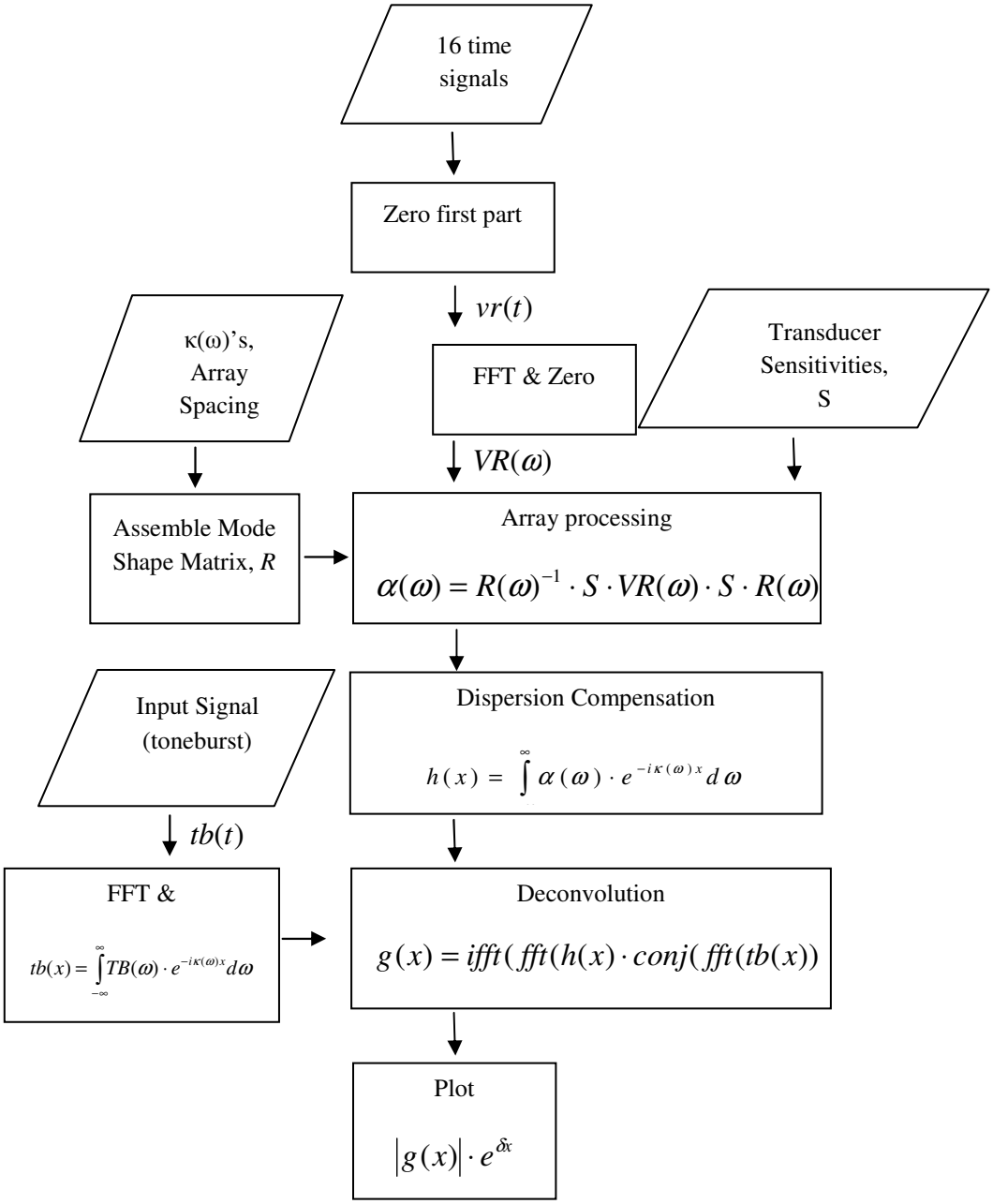

Figure 5 Signal Processing Algorithm.

The first term in equation 1 contains the received modes for the different excited modes and is expanded in equation 2 at a particular frequency. Here the column superscripts indicate the mode that is targeted for transmission while the row corresponds to the mode targeted for receiving. For example, the term in the third row and first column would correspond to mode 4 being transmitted in the forward direction (4f) and mode 4 in the backward direction being received (4b).

$$\alpha = \begin{bmatrix} \begin{Bmatrix} \alpha_{4f} \\ \alpha_{7f} \\ \alpha_{4b} \\ \alpha_{7b} \end{Bmatrix}^{a^{4f}} & \begin{Bmatrix} \alpha_{4f} \\ \alpha_{7f} \\ \alpha_{4b} \\ \alpha_{7b} \end{Bmatrix}^{a^{7f}} & \begin{Bmatrix} \alpha_{4f} \\ \alpha_{7f} \\ \alpha_{4b} \\ \alpha_{7b} \end{Bmatrix}^{a^{4b}} & \begin{Bmatrix} \alpha_{4f} \\ \alpha_{7f} \\ \alpha_{4b} \\ \alpha_{7b} \end{Bmatrix}^{a^{7b}} \end{bmatrix} \tag{2}$$

The linear superposition of the signals with phase shifts is performed by pre multiplication by the inverse of a matrix (receive processing) and post multiplication by a matrix (transmit processing). These matrices are the mode shape matrix and are the same matrix for transmitting and receiving [8]. The mode shape matrix is assembled from the modes shapes and wavenumbers computed at each frequency from the semi-analytical finite element model of the rail as shown in equation 3.

$$[R(\omega)] = \begin{bmatrix} \psi_1^{4f} e^{-j\kappa_{4f}(\omega)z_1} & \psi_1^{7f} e^{-j\kappa_{7f}(\omega)z_1} & \psi_1^{4b} e^{-j\kappa_{4b}(\omega)z_1} & \psi_1^{7b} e^{-j\kappa_{7b}(\omega)z_1} \\ \psi_2^{4f} e^{-j\kappa_{4f}(\omega)z_2} & \psi_2^{7f} e^{-j\kappa_{7f}(\omega)z_2} & \psi_2^{4b} e^{-j\kappa_{4b}(\omega)z_2} & \psi_2^{7b} e^{-j\kappa_{7b}(\omega)z_2} \\ \psi_3^{4f} e^{-j\kappa_{4f}(\omega)z_3} & \psi_3^{7f} e^{-j\kappa_{7f}(\omega)z_3} & \psi_3^{4b} e^{-j\kappa_{4b}(\omega)z_3} & \psi_3^{7b} e^{-j\kappa_{7b}(\omega)z_3} \\ \psi_4^{4f} e^{-j\kappa_{4f}(\omega)z_4} & \psi_4^{7f} e^{-j\kappa_{7f}(\omega)z_4} & \psi_4^{4b} e^{-j\kappa_{4b}(\omega)z_4} & \psi_4^{7b} e^{-j\kappa_{7b}(\omega)z_4} \end{bmatrix} \tag{3}$$

The 16 measured time signals are transformed to the frequency domain and at each frequency the matrix is assembled as shown in equation 4, where the columns correspond to the transducer that was used for excitation and the rows indicate the transducer used to receive the signal.

$$VR = \begin{bmatrix} \begin{Bmatrix} VR_1 \\ VR_2 \\ VR_3 \\ VR_4 \end{Bmatrix}^{Tx1} & \begin{Bmatrix} VR_1 \\ VR_2 \\ VR_3 \\ VR_4 \end{Bmatrix}^{Tx2} & \begin{Bmatrix} VR_1 \\ VR_2 \\ VR_3 \\ VR_4 \end{Bmatrix}^{Tx3} & \begin{Bmatrix} VR_1 \\ VR_2 \\ VR_3 \\ VR_4 \end{Bmatrix}^{Tx4} \end{bmatrix} \tag{4}$$

The matrices S_R and S_T, in equation 1, are diagonal matrices containing receive and transmit calibration factors of the transducers.

Dispersion Compensation

The group velocity of guided waves is generally frequency dependent. This causes a wave packet to become distorted with distance as different frequency components travel at different speeds. Wilcox [7] developed a technique for removing the effect of dispersion from guided wave signals. The received signal is propagated backwards to time equals zero, which gives the dispersion compensated signal at the transducer as a function of distance to the reflector. For mode α this requires the following integral evaluation at different distances.

$$h(x) = u(-x',0) = \int_{-\infty}^{\infty} \alpha(\omega) \cdot e^{-i\kappa(\omega)x} d\omega \tag{5}$$

An algorithm was presented by Wilcox for quickly evaluating this integral using a fast Fourier transform. This algorithm, which requires the group velocity to be known at each frequency, was implemented and used. The group velocity of the propagating modes is computed from the semi-analytical finite element model and is shown for mode 4 in figure 6. The algorithm also converts the frequency domain signals to distance signals. For example, a portion of the signal obtained when transmitting mode 4 forward and receiving mode 4 backward is shown in figure 6. The signal that would have been obtained if the dispersion compensation had not been used is also shown to illustrate that the process removes some of the distortion of the wave packet.

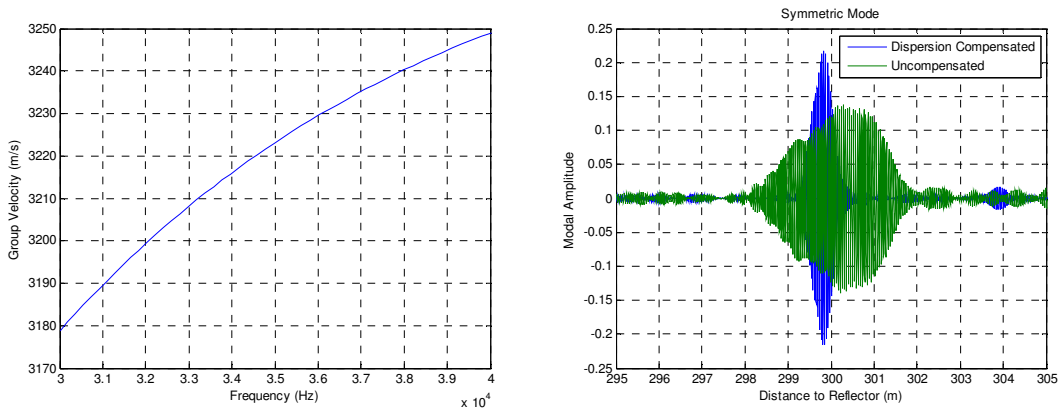

Figure 6 Dispersion compensation using computed group velocity.

PROCESSED MEASUREMENT RESULTS AND DISCUSSION

Results for the transmission and reception of mode 4 are included. Mode 7 did not produce satisfactory results. The final result of the measurement after application of the signal processing algorithm is shown in figure 6.

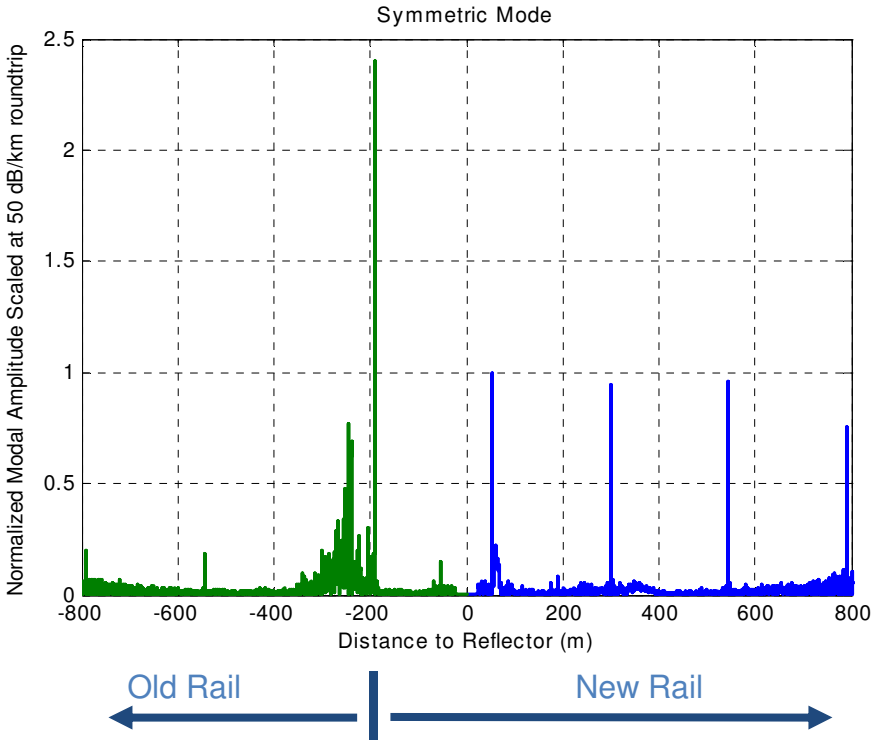

Figure 7 Measured reflections of symmetric mode of propagation after processing.

In figure 7 the array was located at 0m and reflections from either side are shown. In the positive direction we see that there are similar reflections at distances of approximately 50m, 300m, 540m and 790m. It was found that these distances coincided with the distances of thermite welds used to join the rail in the field during installation. Figure 8 shows a photograph of the weld at 300m and a zoomed in view of the measured reflection.

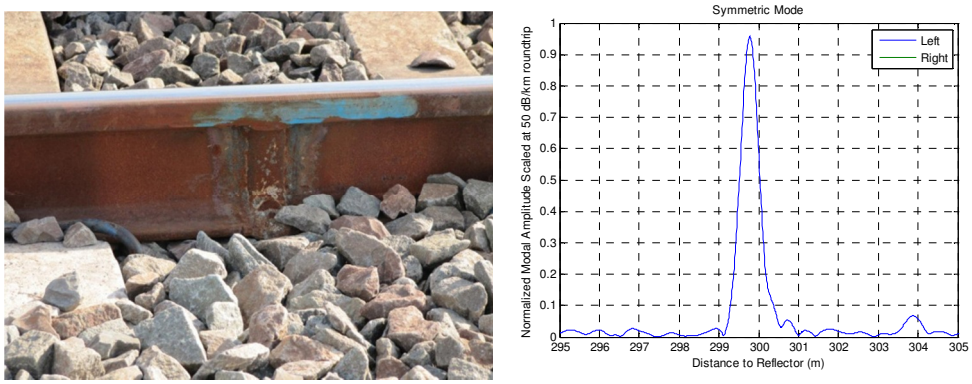

Figure 8 Thermite weld and measured reflection at 300m.

It is evident that the thermite welds are easily detected in new rail and that the range resolution is more than adequate for the purpose of locating defects.

In the negative direction we see that there is a very large reflection at -190m followed by numerous smaller reflections. On inspection it was found that the large reflection was due to a weld joining new rail to old rail as shown in figure 9. The old rail then contained numerous welds sometimes with only 6m between welds. Inspection or monitoring of old rails would only be possible over short ranges.

There appear to be reflections at -50m and -540m. These are actually believed to be ghost reflections from the positive side. These are believed to be due to differences in the performance of the transducers used in the array. The calibration factors of the transducers are unknown and in this work they were assumed to be constant with frequency and the receive sensitivity of the transducer was assumed to be equal to the transmit sensitivity. The sensitivity of the one transducer was set to unity and the remaining three factors were adjusted, by trial and error, until the ghost reflections were minimised. Further work is required to understand this and to develop a technique for calibrating the transducers.

Figure 9 New rail welded to old rail and frequency welds in old rail.

Numerical modelling of the interaction of this guided wave mode with welds and transverse cracks in the rail head has been performed [9]. This modelling indicates that reflections from these cracks should be large relative to the weld reflections. Therefore we expect to be able to detect these cracks prior to rail breakage.

CONCLUSIONS

SAFE model data was used to design a transducer array and a signal processing algorithm to process the measured signals. The performance achieved by the signal processing algorithm provides confidence in the accuracy of the numerical model.

Measurements were performed on a rail section that included both new rail and old rail in very poor condition. The old rail had numerous thermite welds performed in the field and these would make crack detection very difficult and it is thought that the 500 m range would not be achievable. The new rail

included thermite welds every 250 m and these were easily detected up to a distance of 790 m from the transducer array. We expect transverse crack in the rail head to provide stronger reflections before breakage occurs and are therefore confident that these will be detectable at a range of 500 m in rail, which is in relatively good condition.

REFERENCES

1 P. Wilcox, B. Pavlakovic, M. Evans, K. Vine, P. Cawley, M. Lowe, and D. N. Alleyne, "Long range inspection of rail using guided waves," in Review of Progress in Quantitative Nondestructive Evaluation, Volume 22, pp. 236–243, 2003

2 F. A. Burger, "A Practical Continuous Operating Rail Break Detection System Using Guided Waves," in 18th World Conference on Nondestructive Testing, 2012.

3 P. W. Loveday, "Guided Wave Inspection and Monitoring of Railway Track," Journal of Nondestructive Evaluation, vol. 31, no. 4, pp.303-309, 2012.

4 L. Gavric, "Computation of propagative waves in free rail using a finite element technique," Journal of Sound and Vibration, vol. 185, no. 3, pp. 531–543, Aug. 1995.

5 P. W. Loveday and C. S. Long, "Field measurement of guided wave modes in rail track," in Review of Progress in Quantitative Nondestructive Evaluation, vol. 32, pp230-237, 2013.

6 P. W. Loveday and C. S. Long, "Measurement of Guided Ultrasonic Waves in Rails," in Proc. Eighth South African Conference on Computational and Applied Mechanics (SACAM 2012), 2012, pp. 88–94.

7 P. D. Wilcox, "A rapid signal processing technique to remove the effect of dispersion from guided wave signals.," IEEE Transactions on Ultrasonics, Ferroelectrics and Frequency Control, vol. 50, no. 4, pp. 419–27, 2003.

8 P. D. Wilcox, "Guided-wave Array Methods," in Encyclopedia of Structural Health Monitoring, 2009.

9 C. S. Long and P. W. Loveday, "Prediction of Guided Wave Scattering by Defects in Rails Using Numerical Modelling," to appear in Review of Progress in Quantitative Nondestructive Evaluation, 2013.

ACKNOWLEDGEMENTS

Access to the railway track for field measurements was provided by Transnet Freight Rail and is gratefully acknowledged. Funding for this project was provided by the CSIR, the Department of Science and Technology and the National Research Foundation of South Africa (Grant No's: 78858 & 85330).